

Geophysical Research Letters®



RESEARCH LETTER

10.1029/2023GL107111

Key Points:

- Borneo stalagmite record shows anomalously low El Niño–Southern Oscillation variability in a 135-year-long window, centered at 4.1 kyBP
- Borneo stalagmite record suggests an abrupt shift from low to high El Niño–Southern Oscillation variability between 3.8 and 4.0 kyBP
- Records of tropical hydroclimate change ~4,000 years ago may reflect a significant increase in El Niño variability

Supporting Information:

Supporting Information may be found in the online version of this article.

Correspondence to:

S. A. Carolin,
stacy.carolin@arch.ox.ac.uk

Citation:

Theaker, C. M., Carolin, S. A., Day, C. C., Cobb, K. M., Chen, S., Grothe, P. R., & Couper, H. O. (2024). Borneo Stalagmite evidence of significantly reduced El Niño–Southern Oscillation variability at 4.1 kyBP. *Geophysical Research Letters*, 51, e2023GL107111. <https://doi.org/10.1029/2023GL107111>

Received 31 OCT 2023

Accepted 4 MAR 2024

Author Contributions:

Conceptualization: C. M. Theaker,

S. A. Carolin, C. C. Day

Formal analysis: C. M. Theaker,

S. A. Carolin, C. C. Day, K. M. Cobb,

S. Chen, P. R. Grothe

Investigation: C. M. Theaker, C. C. Day,

H. O. Couper

Methodology: C. M. Theaker,

S. A. Carolin, C. C. Day

Resources: C. C. Day

Supervision: S. A. Carolin, C. C. Day

Visualization: C. M. Theaker,

S. A. Carolin, P. R. Grothe





Writing – original draft: C. M. Theaker

© 2024. The Authors.

This is an open access article under the terms of the [Creative Commons Attribution-NonCommercial-NoDerivs](https://creativecommons.org/licenses/by/4.0/)

License, which permits use and distribution in any medium, provided the original work is properly cited, the use is non-commercial and no modifications or adaptations are made.

Borneo Stalagmite Evidence of Significantly Reduced El Niño–Southern Oscillation Variability at 4.1 kyBP

C. M. Theaker¹, S. A. Carolin^{1,2,3} , C. C. Day¹ , K. M. Cobb⁴, S. Chen⁵ , P. R. Grothe⁶ , and H. O. Couper¹

¹Department of Earth Sciences, University of Oxford, Oxford, UK, ²Department of Earth Sciences, University of Cambridge, Cambridge, UK, ³Now at School of Archaeology, University of Oxford, Oxford, UK, ⁴Department of Earth, Environmental, and Planetary Sciences, & Environment and Society, Brown University, Providence, RI, USA, ⁵School of Oceanography, Shanghai Jiao Tong University, Shanghai, China, ⁶Earth and Environmental Sciences, University of Mary Washington, Fredericksburg, VA, USA

Abstract The timing and geographic extent of a potential “4.2 ky event” remain highly contested. Here we present records of ENSO variability at 3.8 kyBP and 4.1 kyBP derived from a Borneo stalagmite, which suggest a significant change in ENSO properties between these time intervals. The Borneo records show evidence of significantly reduced ENSO activity at 4.1 kyBP, relative to other measured windows within the Holocene. This reduced ENSO activity coincides with a period of drier conditions and enhanced dust events in the Middle East that took place ~4.0–4.3 kyBP. The Borneo records show evidence of enhanced ENSO activity at 3.8 kyBP. Various hydroclimate changes attributed to the “4.2 ky event” in many regions may thus be reflecting a shift from reduced to enhanced El Niño activity that occurred between 3.8 kyBP to 4.0 kyBP.

Plain Language Summary Research suggests that a significant climate shift may have occurred around 4,000 years ago, though the exact timing and global extent of the event remain uncertain. A change in the frequency or magnitude of the El Niño–Southern Oscillation (ENSO) is one hypothesized cause, however there are currently few high-resolution records which resolve ENSO variability 4,000 years ago. We present a new western tropical Pacific stalagmite-based record of ENSO activity, which shows a significant minimum in ENSO variability around 4,100 years ago. This reduced ENSO activity coincides with a centennial-scale climate event in the Middle East characterized by drier conditions and enhanced dust events. The Borneo record also shows a significant increase in El Niño/La Niña activity that took place by 3,800 years ago. Hydroclimate changes around 4,000 years ago found in records from multiple regions around the world may therefore reflect a shift from reduced to enhanced El Niño activity.

1. Introduction

Records in several regions around the world, including tropical Africa and tropical South America (e.g., Marchant & Hooghiemstra, 2004), south Asia (e.g., Kathayat et al., 2017, 2018), and the Middle East (e.g., Carolin et al., 2019; Cullen et al., 2000; Sharifi et al., 2015; Watanabe et al., 2019) document hydroclimate anomalies which occurred approximately 4,000 years ago (4 kyBP; kiloyears before 1950 CE). The significance of the 4 kyBP period is reflected in its selection as the chronostratigraphic boundary between the Northgrippian and Meghalayan subdivisions of the Holocene epoch (Walker et al., 2018), though the exact timing and global extent of a centennial-scale event at this time, and its climatic driver, remain highly contested (e.g., Bini et al., 2019; Bradley & Bakke, 2019; Kathayat et al., 2018; Railsback et al., 2018; Voosen, 2018; Ön et al., 2021).

The tropics-wide evidence for major climate and environmental changes around 4 kyBP has led several authors to hypothesize that a shift in the frequency or magnitude of El Niño–Southern Oscillation (ENSO) events, and/or a change in the mean state of the tropical Pacific, may underlie documented changes at this time (Booth et al., 2005; Dang et al., 2020; Li et al., 2018; Marchant & Hooghiemstra, 2004; Renssen, 2022; Scroton et al., 2023; Toth & Aronson, 2019; Wang et al., 2022). The small number of multi-millennium records of ENSO variability do indeed document a trend toward higher variability from the mid-to late-Holocene (e.g., Carré et al., 2014, 2021; Conroy et al., 2008; Du et al., 2021; Emile-Geay et al., 2016; Koutavas & Joanides, 2012; Lawman et al., 2022). However, there are few available high-resolution records capable of resolving the precise timing and magnitude of any centennial-scale ENSO variability shifts around 4.0 kyBP (McGregor et al., 2013; Cobb et al., 2013; Dang et al., 2020; X. Chen et al., 2023).

Writing – review & editing:

C. M. Theaker, S. A. Carolin, C. C. Day,
K. M. Cobb, S. Chen, P. R. Grothe,
H. O. Couper

While tropical Pacific corals are excellent recorders of ENSO anomalies (e.g., Cobb et al., 2003; Cobb et al., 2013; Evans et al., 1999; Kilbourne et al., 2004; McGregor et al., 2013; McGregor & Gagan, 2004; Tudhope et al., 2001; Woodroffe & Gagan, 2000), fossil coral lengths typically span just a few decades (e.g., Grothe et al., 2020), which complicates the identification of centennial to millennial scale trends in ENSO given the high level of internal ENSO variability (Emile-Geay et al., 2016). S. Chen et al. (2016) demonstrated the benefits of tropical stalagmites (e.g., Frappier et al., 2002; Liu et al., 2018) as an alternative archive for ENSO reconstruction, which allow for the generation of century-long, high-resolution windows across specific time periods of interest, anchored to high-precision U/Th dates.

Mulu National Park in Borneo (4.25°N, 114.96°E, Figure S1 in Supporting Information S1), which contains multiple limestone outcrops with hundreds of kilometers of cave passages, sits in the center of the Indo-Pacific Warm Pool, with interannual rainfall variability primarily controlled by ENSO (Ellis et al., 2020; Moerman et al., 2013) (Figure 1). Monitoring from 2006 to 2018 shows Mulu rainwater $\delta^{18}\text{O}$ strongly responded both to the 2009–2010 Central Pacific El Niño event (Takahashi et al., 2011) and to the Central-to-East Pacific (middle of the ENSO continuum) 2015–2016 El Niño event (L'Heureux et al., 2017) (Figure 1). Mulu's Gunung Api cave dripwater $\delta^{18}\text{O}$ is strongly correlated with Mulu rainfall $\delta^{18}\text{O}$ changes across ENSO extremes (Figure 1; Moerman et al., 2014; Ellis et al., 2020), with reduced dripwater $\delta^{18}\text{O}$ amplitudes and longer lags associated with longer karst transit times (Moerman et al., 2014). Modeling shows there is no significant reduction in interannual variance in the dripwater $\delta^{18}\text{O}$ record unless the dripwater residency time is increased to greater than 18 months (Moerman et al., 2014; S. Chen et al., 2016). Gunung Api dripwater $\delta^{18}\text{O}$ residence time is calculated as between 3 and 10 months based on over 10 years of dripwater monitoring at three different drips (Ellis et al., 2020;

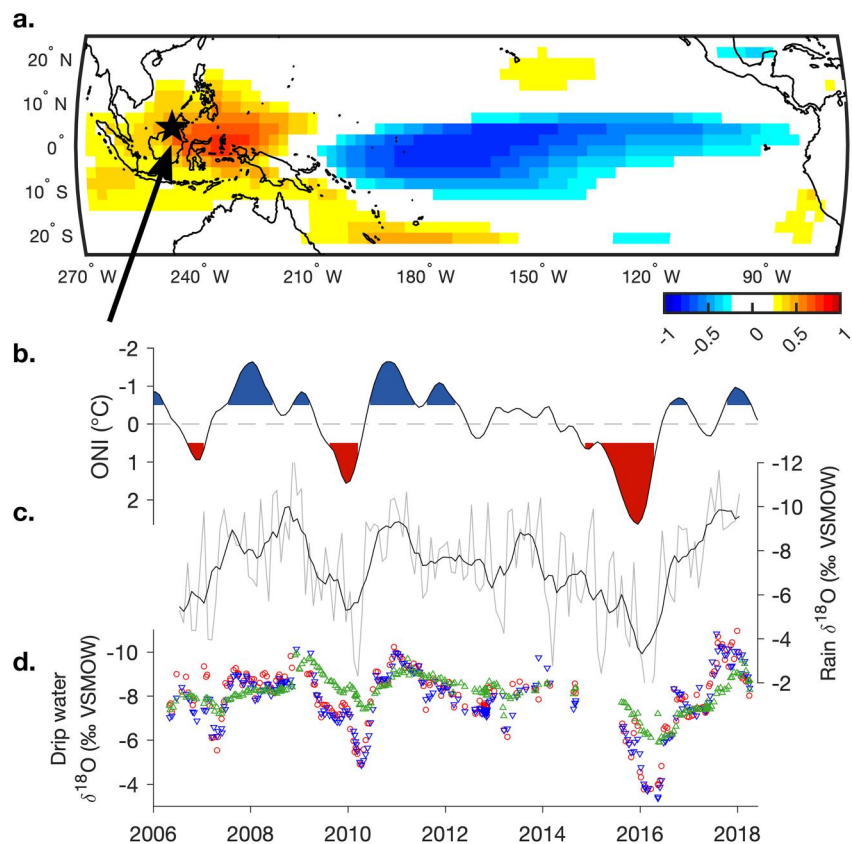


Figure 1. Modern El Niño—Southern Oscillation (ENSO) conditions at our study site in northern Borneo. (a) Spatial correlation between the Oceanic Niño Index and 3-month running average outgoing long wave (OLR) radiation, a metric for convective activity. Location of the study site is marked with a black star. (b) Oceanic Niño Index. Red (blue) coloring indicates warm (cold) ENSO anomalies based on a threshold of +0.5°C (−0.5°C). (c) Mulu monthly rainfall $\delta^{18}\text{O}$ (gray) with a 7-month running mean (black line) (Ellis et al., 2020; Moerman et al., 2013). (d) Collected Mulu cave drip water $\delta^{18}\text{O}$ from three sites: Wind Cave Fast (red), Wind Cave Slow (blue), and Lang's Cave (green) (Ellis et al., 2020; Moerman et al., 2014).

Moerman et al., 2014). Thus, in the absence of any evidence of a large change in water residence time, stalagmite $\delta^{18}\text{O}$ records from this site can be used as a proxy for ENSO variability.

S. Chen et al. (2016) presented estimates of ENSO variability in six discrete intervals of the Holocene (60–200 years duration) using sub-annual resolution $\delta^{18}\text{O}$ records measured from Borneo stalagmite BA03. Stalagmite BA03 was collected in 2003 from Bukit Assam—in the same geologic formation Gunung Api is located (Figure S1 in Supporting Information S1)—under permits approved by Malaysia and Sarawak. The sub-annual BA03 $\delta^{18}\text{O}$ records were interpolated to a resolution of two samples per year and the power spectra were analyzed to confirm significant interannual variability above 95% red noise. The records were filtered using a 2–7 years band pass wavelet filter, and the standard deviations of the filtered records were calculated to quantify interannual variability associated with ENSO in each window. While the BA03 windows presented by S. Chen et al. (2016) showed a significant reduction in interannual variability during the mid-Holocene—results supported by other records from the central and eastern Pacific (Carré et al., 2014, 2021; Conroy et al., 2008; Grothe et al., 2020; Koutavas & Joanides, 2012; McGregor et al., 2013)—questions regarding the abruptness of a shift in ENSO variability across the mid-to late-Holocene boundary, a period which potentially includes a ‘4.2 kyBP event,’ remain unanswered.

Here we present two new long-duration (>100 years) sub-annual BA03 $\delta^{18}\text{O}$ records, centered at 3.8 kyBP and 4.1 kyBP. The records allow for the investigation of centennial-scale changes in ENSO variability that took place coincident with and immediately following the purported “4.2 ky event,” accounting for chronological error with an ensemble-based approach to the U/Th age model. The results are compared with other high-resolution, precisely dated records that resolve ENSO variability within the 3.5–4.5 kyBP period. We show that reconstructions of ENSO variability derived from central and western Pacific archives document systematic and significant changes around the “4.2 ky event” period, and discuss the implications of these results.

2. Materials and Methods

Stalagmite BA03 grew relatively continuously through the Holocene (Figure S2 in Supporting Information S1) with a basal age of 11.63 kyBP (S. Chen et al., 2016). We replicated the S. Chen et al. (2016) methodology to generate sub-annually resolved (average sampling resolution equates to ~ 3 samples/yr) stalagmite $\delta^{18}\text{O}$ records for estimation of ENSO variability in two new >100 year-length windows centered at 3.8 kyBP and 4.1 kyBP (Supporting Information S1). The specific placements of the windows were chosen by targeting locations in the stalagmite around 4.0 kyBP which have the greatest age model precision due to bracketing U-Th ages with low uncertainties. Construction of a sub-annually resolved stalagmite $\delta^{18}\text{O}$ record immediately prior to 4.3 kyBP was not possible due to the high detrital Th contamination in this section, which reduced the accuracy of the associated U-Th ages.

Stalagmite calcite was milled at either 50 or 60 μm increments (sub-annual temporal resolution) in two continuous trenches along the stalagmite growth axis (Figure S3 in Supporting Information S1). A total of 715 calcite powders were analyzed on a Thermo Delta V Advantage Isotope Ratio Mass Spectrometer ($\delta^{18}\text{O}$ reproducibility of an in-house marble standard on individual runs ranged from $\pm 0.05\text{‰}$ to $\pm 0.06\text{‰}$, 1σ) (Supporting Information S1). The BA03 age model was developed using the OxCal Bayesian method P-sequence Deposition model (Bronk Ramsey, 2008; Bronk Ramsey & Lee, 2013) (further details in Supporting Information S1), using the same 36 U-Th dates presented in S. Chen et al. (2016) (Table S1 in Supporting Information S1). Due to BA03's relatively constant growth rate through the Holocene, the OxCal mean age model is similar to the StalAge-derived (Scholz & Hoffmann, 2011) mean age model applied in S. Chen et al. (2016), except for the 5.2 kyBP window period, which has poor age model precision (Figure S5 in Supporting Information S1). We tested the effect of chronological uncertainty on the calculated BA03 ENSO estimates using multiple age models constructed from both classical interpolation and Bayesian methods.

3. Results

This study presents Borneo stalagmite-derived ENSO variability estimates in two new windows centered at 3.8 kyBP (104-year duration window) and 4.1 kyBP (135-year duration window). The temporal resolution for the two records is 0.33 ± 0.07 (95% CI) yr/sample (Figure S6 in Supporting Information S1). Multi-taper spectral analysis of each $\delta^{18}\text{O}$ time-series shows at least one peak above the 95% confidence limit of the red noise background within the 2–7 year periodicity ENSO band, though the 4.1 kyBP spectra is somewhat more muted across the

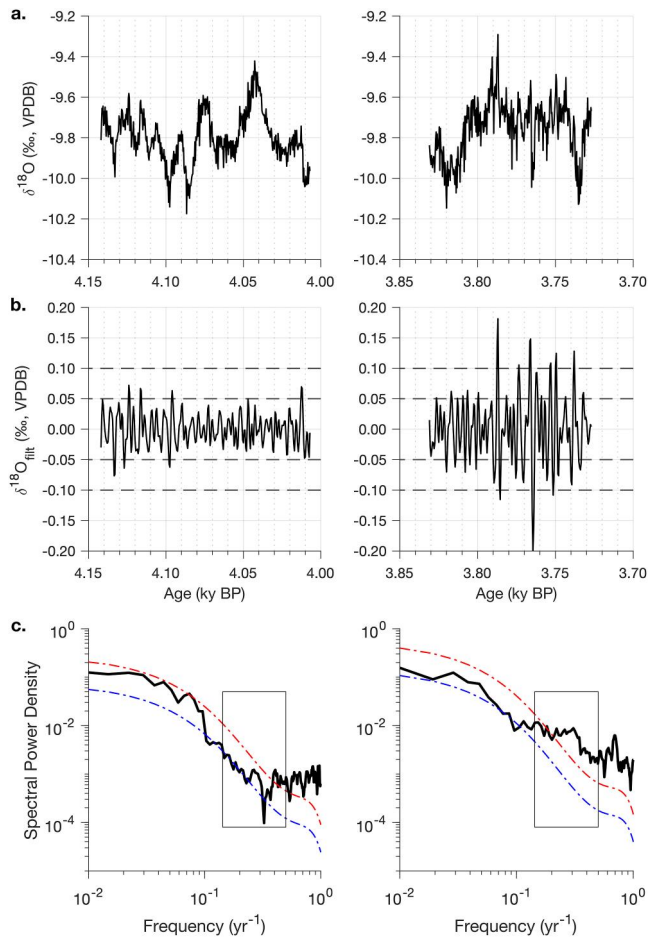


Figure 2. Stalagmite BA03 high resolution $\delta^{18}\text{O}$ records in 3.8 kyBP and 4.1 kyBP windows. (a) $\delta^{18}\text{O}$ records on the OxCal age model. (b) Bandpass (2–7 year) filtered $\delta^{18}\text{O}$ records (see Supporting Information S1 for detailed methods on filtering). (c) Power spectra of the 4.1 kyBP $\delta^{18}\text{O}$ record (left) and 3.8 kyBP $\delta^{18}\text{O}$ record (right). The blue and red dashed lines represent the mean and 95% confidence limit of the power spectra of 100 generated red noise time-series, respectively. The black box outline marks the 2–7 year band of ENSO periodicities.

4.1 kyBP window variance is significantly lower ($p < 0.05$) than the full 3.8 kyBP window variance in 78.9% of the 1,000 records tested on individual ensemble OxCal age models, and 98.1% of the 1,000 records tested on individual ensemble COPRA age models.

4. Discussion

The new BA03 estimates of ENSO variability present the strongest evidence to date of a significant, large shift from reduced ENSO variability prior to 4 kyBP, to enhanced ENSO variability post 4 kyBP, which occurs within a few centuries. The shift from reduced to enhanced ENSO variability at the 4 kyBP boundary is more abrupt than previously shown in other paleo-ENSO archives (e.g., Conroy et al., 2008; Koutavas & Joanides, 2012; Carré et al., 2014; S. Chen et al., 2016). Orbital variations which cause seasonal insolation strength changes have been suggested by many authors as a possible forcing responsible for the observed changes in ENSO variability strength through the Holocene (e.g., S. Chen et al., 2016; Emile-Geay et al., 2016; Carré et al., 2021; Lawman et al., 2022). The more abrupt decadal to centennial-scale shift in ENSO variability recorded in BA03 around 4 kyBP may be reflecting processes internal to the climate system at shorter timescales, as already evidenced in the coral records at other times through the Holocene (Cobb et al., 2013; Grothe et al., 2020).

ENSO frequencies (Figure 2). The spectral power density of the ONI index and of all BA03 windows, including those previously published, is shown in Figure S7 in Supporting Information S1.

BA03 element-to-calcium ratios which were measured at approximately decadal-scale resolution from 3.6 to 4.8 kyBP show no indication of a significant change in dripwater karst residence time through this period. These results add further assurance that the $\delta^{18}\text{O}$ interannual variability measured in BA03 at 3.8 kyBP and 4.1 kyBP reflects changes in rainwater $\delta^{18}\text{O}$ linked to ENSO variability, not karst dripwater processes.

The 4.1 kyBP period presents the longest duration low ENSO variability window of the Holocene derived from the BA03 stalagmite ENSO archive (Figure 3). A single 50-year ENSO variability estimate centered at 8.2 kyBP is the only other period of similarly low ENSO variability measured in the BA03 Holocene windows (Figure S8 in Supporting Information S1). Results of a block-bootstrap test of equal variance confirm that the full 4.1 kyBP window variance is significantly lower ($p < 0.01$) than all other BA03 windows, when adjusted for equivalent window duration (Table S3 in Supporting Information S1). Further, the high ENSO variability value centered at 3.8 kyBP now precisely constrains an end to the mid-Holocene low-ENSO period (S. Chen et al., 2016; Emile-Geay et al., 2016). The shift from a period of minimum ENSO variability centered at 4.1 kyBP (>100-year duration) to a period of high ENSO variability centered at 3.8 kyBP (>100-year duration), occurs within a few centuries, and is the largest shift in ENSO variability across the BA03 reconstructions.

We compare ENSO variability estimates calculated from records on the mean StalAge age model (Scholz & Hoffmann, 2011), the mean plus 1,000 individual ensemble COPRA age models (Breitenbach et al., 2012), and the mean plus 1,000 individual ensemble OxCal age models (Bronk Ramsey, 2008; Bronk Ramsey & Lee, 2013) (Figure 3). The results demonstrate a spread in BA03 ENSO variability estimates for a particular window due to the inherent chronological uncertainty in the stalagmite record (Figure 3). Despite the added ENSO variability estimate uncertainty, the ENSO variability estimate distribution for the window centered at 4.1 kyBP is visibly offset from the neighboring windows' distributions, upholding the conclusion of an anomalously reduced BA03 $\delta^{18}\text{O}$ variability in the 2–7 years band during this period (Figure 3). The block-bootstrap test of equal variance confirms that the full

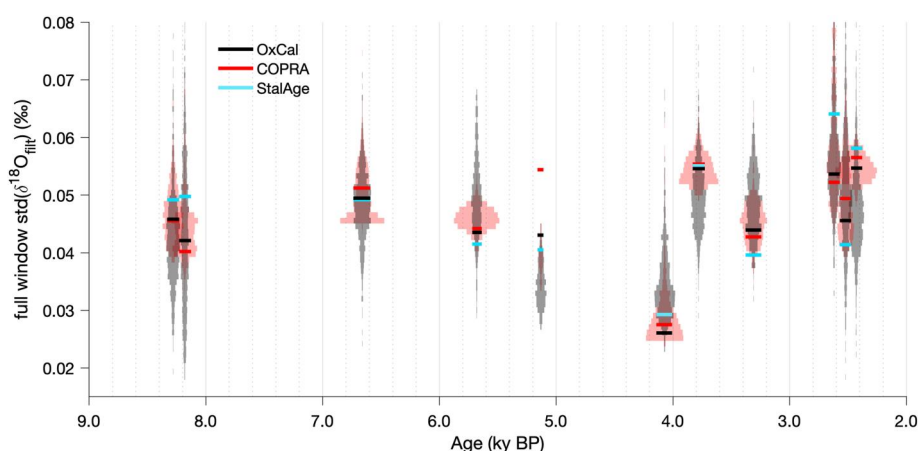


Figure 3. Borneo stalagmite BA03 full-window ENSO variability estimates calculated from $\delta^{18}\text{O}$ records on a multitude of possible age models constructed using the OxCal (black), COPRA (red), and StalAge (blue) programs (references in text). Longer duration windows have been separated into two (8.2 kyBP window) or three (2.5 kyBP window) sections so that all windows span approximately the same duration in time (~ 80 – 140 years). ENSO variability estimates calculated from the mean age model of each program are plotted as thick horizontal lines, with the length of the line equal to each window's duration on the OxCal mean age model. The distribution of ENSO variability estimates calculated from 1,000 OxCal (gray) and COPRA (pink) ensembles are plotted as vertical symmetric histograms, bar width 0.001% . Ensemble ENSO variability estimates from records which span less than 50 years duration are not included in the distribution plots.

The BA03 results agree with ENSO-proxy records derived from Line Island corals (Cobb et al., 2013; McGregor et al., 2013) which also suggest reduced ENSO variability around 4.1 kyBP. Using a modern calibration, the Line Island corals suggest ENSO variability was reduced by 40%–60% in the 4.1–4.3 kyBP period, relative to 1955–2005 C.E (Cobb et al., 2013; Grothe et al., 2020; McGregor et al., 2013). With its multiple >60 years windows of resolved ENSO variability, the BA03 stalagmite record now demonstrates that the 4.1 kyBP reduction in ENSO variability is unmatched when compared to several periods throughout the early, mid, and late Holocene. The only period with a similar reduction in interannual $\delta^{18}\text{O}$ variability is a single 50-year period centered at 8.2 kyBP (Figure S8 in Supporting Information S1).

A collection of corals from the northern South China Sea (SCS) grew within the 4.1–4.5 kyBP window and indicate cooler and possibly wetter conditions at this time (Dang et al., 2020; X. Chen et al., 2023). One study hypothesizes that the SCS coral records indicate weak ENSO intensity (Dang et al., 2020), while a second study suggests the SCS data, combined with the Line Island coral records, indicates more frequent Central Pacific (CP) El Niño events relative to East Pacific (EP) El Niño events (X. Chen et al., 2023), citing the Community Earth System Model v1 (CESM1) simulation results from Karamperidou and DiNezio (2022). From the 2006–2018 Mulu rainwater $\delta^{18}\text{O}$ monitoring alone, it is not yet clear if CP and EP El Niño events influence Mulu rainwater $\delta^{18}\text{O}$ differently. As such, the new BA03 records currently neither support nor reject the hypothesis of more frequent CP El Niño events relative to EP El Niño events to justify the observed reduced interannual variability around 4.2 kyBP in the central Pacific coral and now west Pacific stalagmite $\delta^{18}\text{O}$ records.

The “4.2 kyBP event” was originally named in the early 1990s in recognition of a suggested northern Mesopotamia drought event (Weiss et al., 1993). Since that time multiple proxy records have been published which do indeed verify enhanced winter and summer Shamal dust events and anomalously dry conditions in the Middle East region from ~ 4.0 to 4.3 kyBP (Carolin et al., 2019; Cullen et al., 2000; Sharifi et al., 2015; Watanabe et al., 2019). Modern meteorological data suggests a possible relationship between regional dust events and ENSO (e.g., Huang et al., 2021). Arabian Peninsula dust activity from 1975 to 2012, for example, was found to be associated with anomalously cool tropical east Pacific SSTs on interannual timescales (Y. Yu et al., 2015). Winter-to-spring La Niña conditions correlate with decreased rainfall across the primary dust source region of the Arabian Peninsula, and anticyclonic circulation over the central Arabian Peninsula enhances the Shamal winds (Y. Yu et al., 2015; Huang et al., 2021). The central Pacific coral and west Pacific stalagmite records' reduced interannual variability around 4.2 kyBP may be reflective of conditions in the tropical Pacific favorable to more frequent dust events in the Middle East at this time.

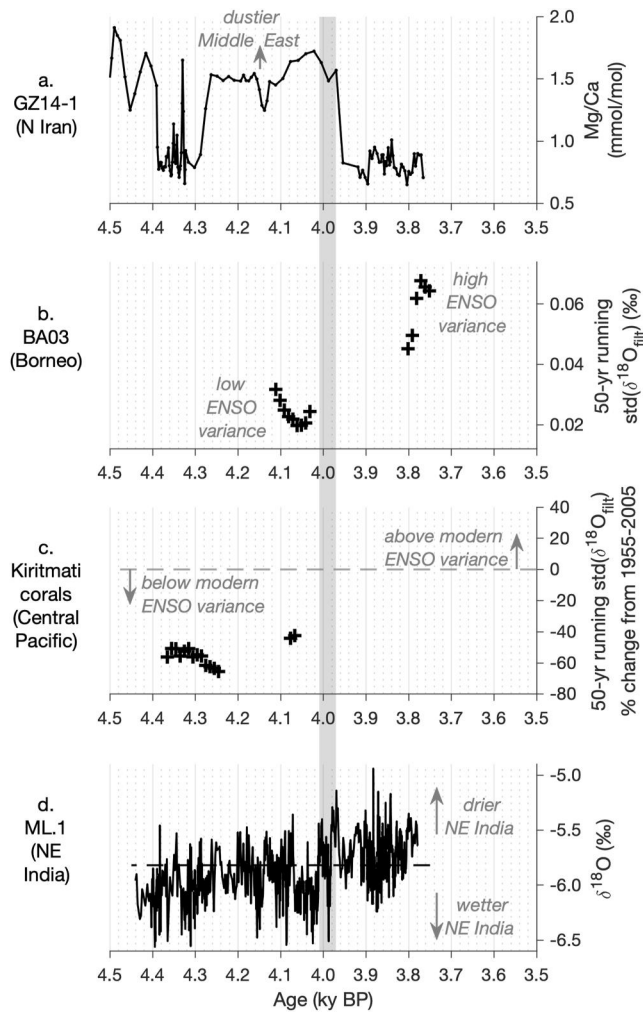


Figure 4. Estimates of ENSO variability compared with dust events in the Middle East and ISM strength in NE India. Gray bar is placed at 4.0 kyBP to highlight the suggested approximate timing of the shift from low to high ENSO variability. (a) Stalagmite GZ14-1 Mg/Ca (mmol/mol), a proxy for dust events in the Middle East (Carolin et al., 2019). (b) Borneo stalagmite BA03 ENSO variability estimates, 50-year running standard deviations at 10-year steps (this study). (c) Kiritmati fossil coral XM35 (mean age 4.31 kyBP, 175 years duration, McGregor et al., 2013) and P34 (mean age 4.07 kyBP, 68 years duration, Cobb et al., 2013) ENSO variability estimates, plotted as the percentage change from modern variance (1955–2005 CE), 50-year running standard deviations at 10-year steps (modified from Grothe et al., 2020, Figure S18b in Supporting Information S1). (d) Stalagmite ML.1 $\delta^{18}\text{O}$, a proxy for ISM strength in NE India. Dashed line is the mean of all $\delta^{18}\text{O}$ values in the record (Kathayat et al., 2018).

Niño Index (ONI), a 3 month running mean of ERSST.v5 (Huang et al., 2017) SST anomalies in the Niño 3.4 region (5°N – 5°S , 120° – 170°W), data set is provided by the US National Weather Service Climate Prediction Center (NWS CPC, 2023). The Mulu rainwater and drip water data are found in the supplemental tables of Moerman et al. (2013, 2014) and Ellis et al. (2020). The Line Island coral data are found in the Grothe et al. (2020) supplement. The GZ14-1 (Carolin et al., 2019) and ML.1 (Kathayat et al., 2018) stalagmite data are found in the sisalv2 database (Comas-Bru et al., 2020).

Global patterns of hydroclimate anomalies found in South America (wet), tropical Africa (dry), and south Asia (dry) around 4 kyBP, also linked by several authors to the “4.2 ky event,” are characteristic of El Niño event signatures (e.g., Renssen, 2022). We suggest these signals may be reflecting a shift to a period characterized by the presence of strong El Niño events which began post 4 kyBP (Figure 4). Marchant and Hooghiemstra (2004) originally reviewed the environmental changes in Africa and South America around 4 kyBP and proposed that the signature reflected a response to changes in Pacific SST and the establishment of El Niño conditions. The observed changes are demonstrated in numerous swamp and lake catchments, but the chronology is not precise. South Asia and the Indian Ocean region, however, have multiple high-resolution, precisely dated hydroclimate records. These records exhibit a common trend toward drier conditions beginning around 4 kyBP (Sroxtton et al., 2023). North and northeast Indian stalagmite $\delta^{18}\text{O}$ records, for example, suggest a shift from wet to dry conditions within the 4.0–4.1 period, dry conditions which then continue for multiple centuries (Kathayat et al., 2017, 2018) (Figure 4). This inferred shift to weak Indian Summer Monsoon (ISM) conditions around 4 kyBP is supported by a lower-resolution nearby lake sediment core hydroclimate record (Dixit et al., 2014). Over long periods, El Niño years are generally associated with below-average Indian monsoon rainfall (e.g., Ihara et al., 2007; Mooley & Parthasarathy, 1983), thus the shift to drier conditions in the Indian monsoon paleorecord may be reflective of stronger or more frequent El Niño events post 4.0 kyBP. MacDonald (2011) previously hypothesized an ISM-ENSO relationship when interpreting monsoon rainfall records related to the Harappan civilization through the Holocene. We note that recent, robustly dated proxy records which record both ISM and Indian Winter Monsoon (IWM) strength in the Indus River valley are interpreted to indicate a weaker ISM and IWM from 4.0 to 4.2 kyBP, and a stronger ISM from 3.6 to 4.0 kyBP (Giesche et al., 2019, 2023). The strong ISM from 3.6 to 4.0 kyBP does not reflect a negative correlation with the Borneo record's suggested high ENSO variability (strong El Niño events) beginning around 4.0 kyBP, highlighting the complex nature of and likely multiple influences on ISM strength across India, apart from just ENSO.

Data Availability Statement

All BA03 data produced for this study are made publicly available on the University of Oxford Research Archive (Theaker et al., 2024). Data will also be added to the NOAA NCEI Paleoclimatology data archive (<https://www.ncei.noaa.gov/products/paleoclimatology>) and the Speleothem Isotope Synthesis and AnaLysis (SISAL) database. BA03 data published in S. Chen et al. (2016) are available at <https://www.ncei.noaa.gov/access/paleo-search/study/19885>. The OLR data set (Liebmann & Smith, 1996) is provided by the US NOAA Physical Sciences Laboratory (NOAA PSL, 2023). The Oceanic

Acknowledgments

We wish to thank all the staff, freelance guides, and locals at Gunung Mulu National Park for their assistance in field work and sample collection over the past 15+ years, specifically Syria Lejau and Jenny Malang. BA03 was collected in the field in 2003 by Jess Adkins and Kim Cobb. Thank you to David Lund and Sharon Hoffman for supplying the sample for this study. Thank you to Gideon Henderson and Franziska Lechleitner for their helpful comments in discussion of this work. Thank you to the reviewers and editor for their time and comments. This work was supported by NERC Doctoral Training Partnership (UK) funds awarded to Christopher Theaker, NERC NEIF project support awarded to Christopher Day, and a National Key Research and Development Program of China Grant 2023YFF0805300 awarded to Sang Chen.

References

- Bini, M., Zanchetta, G., Perşoiu, A., Cartier, R., Català, A., Cacho, I., et al. (2019). The 4.2 kaBP event in the Mediterranean region: An overview. *Climate of the Past*, 15(2), 555–577. <https://doi.org/10.5194/cp-15-555-2019>
- Booth, R. K., Jackson, S. T., Forman, S. L., Kutzbach, J. E., Bettis, E. A., Kreigs, J., & Wright, D. K. (2005). A severe centennial-scale drought in midcontinental North America 4200 years ago and apparent global linkages. *The Holocene*, 15(3), 321–328. <https://doi.org/10.1191/0959683605hl825ft>
- Bradley, R. S., & Bakke, J. (2019). Is there evidence for a 4.2 ka BP event in the northern North Atlantic region? *Climate of the Past*, 15(5), 1665–1676. <https://doi.org/10.5194/cp-15-1665-2019>
- Breitenbach, S. F. M., Rehfeld, K., Goswami, B., Baldini, J. U. L., Ridley, H. E., Kennett, D. J., et al. (2012). Constructing proxy records from age models (COPRA). *Climate of the Past*, 8(5), 1765–1779. <https://doi.org/10.5194/cp-8-1765-2012>
- Bronk Ramsey, C. (2008). Deposition models for chronological records. *Quaternary Science Reviews*, 27(1–2), 42–60. <https://doi.org/10.1016/j.quascirev.2007.01.019>
- Bronk Ramsey, C., & Lee, S. (2013). Recent and planned developments of the program OxCal. *Radiocarbon*, 55(02), 720–730. <https://doi.org/10.1017/S003822200057878>
- Carolin, S. A., Walker, R. T., Day, C. C., Ersek, V., Sloan, R. A., Dee, M. W., et al. (2019). Precise timing of abrupt increase in dust activity in the Middle East coincident with 4.2 ka social change. *Proceedings of the National Academy of Sciences of the United States of America*, 116(1), 67–72. <https://doi.org/10.1073/pnas.1808103115>
- Carré, M., Braconnot, P., Elliot, M., d'Agostino, R., Schurer, A., Shi, X., et al. (2021). High-resolution marine data and transient simulations support orbital forcing of ENSO amplitude since the mid-Holocene. *Quaternary Science Reviews*, 268, 107125. <https://doi.org/10.1016/j.quascirev.2021.107125>
- Carré, M., Sachs, J. P., Purca, S., Schauer, A. J., Braconnot, P., Falcón, R. A., et al. (2014). Holocene history of ENSO variance and asymmetry in the eastern tropical Pacific. *Science*, 345(6200), 1045–1048. <https://doi.org/10.1126/science.1252220>
- Chen, S., Hoffmann, S. S., Lund, D. C., Cobb, K. M., Emile-Geay, J., & Adkins, J. F. (2016). A high-resolution speleothem record of western equatorial Pacific rainfall: Implications for Holocene ENSO evolution. *Earth and Planetary Science Letters*, 442, 61–71. <https://doi.org/10.1016/j.epsl.2016.02.050>
- Chen, X., Deng, W., Xiao, H., Guo, H., Zeng, T., Zhao, J., & Wei, G. (2023). Coral paleoclimate perspectives support the role of low-latitude forcing on the 4.2 ka BP event. *Geophysical Research Letters*, 50(13), e2023GL104010. <https://doi.org/10.1029/2023GL104010>
- Cobb, K. M., Charles, C. D., Cheng, H., & Edwards, R. L. (2003). El Niño/Southern Oscillation and tropical Pacific climate during the last millennium. *Nature*, 424(6946), 271–276. <https://doi.org/10.1038/nature01779>
- Cobb, K. M., Westphal, N., Sayani, H. R., Watson, J. T., Di Lorenzo, E., Cheng, H., et al. (2013). Highly variable El Niño–Southern Oscillation throughout the Holocene. *Science*, 339(6115), 67–70. <https://doi.org/10.1126/science.1228246>
- Comas-Bru, Laia, A., Kamolpat, H., & Sandy and SISAL working group members. (2020). SISAL (Speleothem Isotopes Synthesis and AnaLysis Working Group) database version 2.0 [Dataset]. *University of Reading*. <https://doi.org/10.17864/1947.256>
- Conroy, J. L., Overpeck, J. T., Cole, J. E., Shanahan, T. M., & Steinitz-Kannan, M. (2008). Holocene changes in eastern tropical Pacific climate inferred from a Galápagos lake sediment record. *Quaternary Science Reviews*, 27(11–12), 1166–1180. <https://doi.org/10.1016/j.quascirev.2008.02.015>
- Cullen, H. M., de Menocal, P. B., Hemming, S., Hemming, G., Brown, F. H., Guilderson, T., & Sirocko, F. (2000). Climate change and the collapse of the Akkadian empire: Evidence from the deep sea. *Geology*, 28(4), 379. [https://doi.org/10.1130/0091-7613\(2000\)28<379:CCATCO>2.0.CO;2](https://doi.org/10.1130/0091-7613(2000)28<379:CCATCO>2.0.CO;2)
- Dang, S., Yu, K., Tao, S., Han, T., Zhang, H., & Jiang, W. (2020). El Niño/Southern Oscillation during the 4.2 ka event recorded by growth rates of corals from the North South China Sea. *Acta Oceanologica Sinica*, 39(1), 110–117. <https://doi.org/10.1007/s13131-019-1520-5>
- Dixit, Y., Hodell, D. A., & Petrie, C. A. (2014). Abrupt weakening of the summer monsoon in northwest India 4100 yr ago. *Geology*, 42(4), 339–342. <https://doi.org/10.1130/G35236.1>
- Du, X., Hendy, I., Hinnov, L., Brown, E., Zhu, J., & Poulsen, C. J. (2021). High-resolution interannual precipitation reconstruction of Southern California: Implications for Holocene ENSO evolution. *Earth and Planetary Science Letters*, 554, 116670. <https://doi.org/10.1016/j.epsl.2020.116670>
- Ellis, S. A., Cobb, K. M., Moerman, J. W., Partin, J. W., Bennett, A. L., Malang, J., et al. (2020). Extended cave drip water time series captures the 2015–2016 El Niño in Northern Borneo. *Geophysical Research Letters*, 47(5). <https://doi.org/10.1029/2019GL086363>
- Emile-Geay, J., Cobb, K. M., Carré, M., Braconnot, P., Leloup, J., Zhou, Y., et al. (2016). Links between tropical Pacific seasonal, interannual and orbital variability during the Holocene. *Nature Geoscience*, 9(2), 168–173. <https://doi.org/10.1038/ngeo2608>
- Evans, M. N., Fairbanks, R. G., & Rubenstone, J. L. (1999). The thermal oceanographic signal of El Niño reconstructed from a Kiritimati Island coral. *Journal of Geophysical Research*, 104(C6), 13409–13421. <https://doi.org/10.1029/1999JC900001>
- Frappier, A., Sahagian, D., González, L. A., & Carpenter, S. J. (2002). El Niño events recorded by stalagmite carbon isotopes. *Science*, 298(5593), 565. <https://doi.org/10.1126/science.1076446>
- Giesche, A., Hodell, D. A., Petrie, C. A., Haug, G. H., Adkins, J. F., Plessen, B., et al. (2023). Recurring summer and winter droughts from 4.2–3.97 thousand years ago in north India. *Communications Earth & Environment*, 4(1), 103. <https://doi.org/10.1038/s43247-023-00763-z>
- Giesche, A., Staubwasser, M., Petrie, C. A., & Hodell, D. A. (2019). Indian winter and summer monsoon strength over the 4.2 ka BP event in foraminifer isotope records from the Indus River delta in the Arabian Sea. *Climate of the Past*, 15(1), 73–90. <https://doi.org/10.5194/cp-15-73-2019>
- Grothe, P. R., Cobb, K. M., Liguori, G., Di Lorenzo, E., Capotondi, A., Lu, Y., et al. (2020). Enhanced El Niño–Southern Oscillation variability in recent decades. *Geophysical Research Letters*, 47(7). <https://doi.org/10.1029/2019GL083906>
- Huang, B., Thorne, P. W., Banzon, V. F., Boyer, T., Chepurin, G., Lawrimore, J. H., et al. (2017). Extended reconstructed sea surface temperature, version 5 (ERSSTv5): Upgrades, validations, and intercomparisons. *Journal of Climate*, 30(20), 8179–8205. <https://doi.org/10.1175/JCLI-D-16-0836.1>
- Huang, Y., Liu, X., Yin, Z., & An, Z. (2021). Global impact of ENSO on dust activities with emphasis on the key region from the Arabian Peninsula to Central Asia. *Journal of Geophysical Research: Atmospheres*, 126(9). <https://doi.org/10.1029/2020JD034068>
- Ihara, C., Kushnir, Y., Cane, M. A., & De La Peña, V. H. (2007). Indian summer monsoon rainfall and its link with ENSO and Indian Ocean climate indices. *International Journal of Climatology*, 27(2), 179–187. <https://doi.org/10.1002/joc.1394>
- Karamperidou, C., & DiNezio, P. N. (2022). Holocene hydroclimatic variability in the tropical Pacific explained by changing ENSO diversity. *Nature Communications*, 13(1), 7244. <https://doi.org/10.1038/s41467-022-34880-8>

- Kathayat, G., Cheng, H., Sinha, A., Berkelhammer, M., Zhang, H., Duan, P., et al. (2018). Evaluating the timing and structure of the 4.2 ka event in the Indian summer monsoon domain from an annually resolved speleothem record from Northeast India. *Climate of the Past*, 14(12), 1869–1879. <https://doi.org/10.5194/cp-14-1869-2018>
- Kathayat, G., Cheng, H., Sinha, A., Yi, L., Li, X., Zhang, H., et al. (2017). The Indian monsoon variability and civilization changes in the Indian subcontinent. *Science Advances*, 3(12), e1701296. <https://doi.org/10.1126/sciadv.1701296>
- Kilbourne, K. H., Quinn, T. M., Taylor, F. W., Delcroix, T., & Gouriou, Y. (2004). El Niño–Southern Oscillation–related salinity variations recorded in the skeletal geochemistry of a *Porites* coral from Espiritu Santo, Vanuatu. *Paleoceanography*, 19(4), 2004PA001033. <https://doi.org/10.1029/2004PA001033>
- Koutavas, A., & Joannides, S. (2012). El Niño–Southern Oscillation extrema in the Holocene and last glacial maximum. *Paleoceanography*, 27(4). <https://doi.org/10.1029/2012PA002378>
- Lawman, A. E., Di Nezio, P. N., Partin, J. W., Dee, S. G., Thirumalai, K., & Quinn, T. M. (2022). Unraveling forced responses of extreme El Niño variability over the Holocene. *Science Advances*, 8(9), eabm4313. <https://doi.org/10.1126/sciadv.abm4313>
- L'Heureux, M. L., Takahashi, K., Watkins, A. B., Barnston, A. G., Becker, E. J., Di Liberto, T. E., et al. (2017). Observing and predicting the 2015/16 El Niño. *Bulletin of the American Meteorological Society*, 98(7), 1363–1382. <https://doi.org/10.1175/BAMS-D-16-0009.1>
- Li, C.-H., Li, Y.-X., Zheng, Y.-F., Yu, S.-Y., Tang, L.-Y., Li, B.-B., & Cui, Q.-Y. (2018). A high-resolution pollen record from East China reveals large climate variability near the Northgrippian–Meghalayan boundary (around 4200 years ago) exerted societal influence. *Palaeogeography, Palaeoclimatology, Palaeoecology*, 512, 156–165. <https://doi.org/10.1016/j.palaeo.2018.07.031>
- Liebmann, B., & Smith, C. A. (1996). Description of a complete (interpolated) outgoing longwave radiation dataset. *Bulletin of the American Meteorological Society*, 77, 1275–1277.
- Liu, S., Peng, X., Chen, Q., Qin, S., Zhao, J., Feng, Y., et al. (2018). The 1997–1998 El Niño event recorded by a stalagmite from central China. *Quaternary International*, 487, 71–77. <https://doi.org/10.1016/j.quaint.2017.11.026>
- MacDonald, G. (2011). Potential influence of the Pacific Ocean on the Indian summer monsoon and Harappan decline. *Quaternary International*, 229(1–2), 140–148. <https://doi.org/10.1016/j.quaint.2009.11.012>
- Marchant, R., & Hooghiemstra, H. (2004). Rapid environmental change in African and South American tropics around 4000 years before present: A review. *Earth-Science Reviews*, 66(3–4), 217–260. <https://doi.org/10.1016/j.earscirev.2004.01.003>
- McGregor, H. V., Fischer, M. J., Gagan, M. K., Fink, D., Phipps, S. J., Wong, H., & Woodroffe, C. D. (2013). A weak El Niño/Southern Oscillation with delayed seasonal growth around 4,300 years ago. *Nature Geoscience*, 6(11), 949–953. <https://doi.org/10.1038/ngeo1936>
- McGregor, H. V., & Gagan, M. K. (2004). Western Pacific coral $\delta^{18}\text{O}$ records of anomalous Holocene variability in the El Niño–Southern Oscillation. *Geophysical Research Letters*, 31(11), 2004GL019972. <https://doi.org/10.1029/2004GL019972>
- Moerman, J. W., Cobb, K. M., Adkins, J. F., Sodemann, H., Clark, B., & Tuen, A. A. (2013). Diurnal to interannual rainfall $\delta^{18}\text{O}$ variations in northern Borneo driven by regional hydrology. *Earth and Planetary Science Letters*, 369(370), 108–119. <https://doi.org/10.1016/j.epsl.2013.03.014>
- Moerman, J. W., Cobb, K. M., Partin, J. W., Meckler, A. N., Carolin, S. A., Adkins, J. F., et al. (2014). Transformation of ENSO-related rainwater to dripwater $\delta^{18}\text{O}$ variability by vadose water mixing: ENSO variability in dripwater $\delta^{18}\text{O}$. *Geophysical Research Letters*, 41(22), 7907–7915. <https://doi.org/10.1002/2014GL061696>
- Mooley, D. A., & Parthasarathy, B. (1983). Indian summer monsoon and El Niño. *Pure and Applied Geophysics PAGEOPH*, 121(2), 339–352. <https://doi.org/10.1007/BF02590143>
- NOAA. P. S. L. (2023). NOAA interpolated outgoing Longwave radiation (OLR) [Dataset]. *NOAA PSL*. https://downloads.psl.noaa.gov/Datasets/interp_OLR/
- NWS, C. P. C. (2023). Historical El Niño/La Niña episodes (1950–present) [Dataset]. *National Weather Service Climate Prediction Center*. https://origin.cpc.ncep.noaa.gov/products/analysis_monitoring/ensostuff/ONI_v5.php
- Ön, Z. B., Greaves, A. M., Akçer-Ön, S., & Özeren, M. S. (2021). A Bayesian test for the 4.2 ka BP abrupt climatic change event in southeast Europe and southwest Asia using structural time series analysis of paleoclimate data. *Climatic Change*, 165(1–2), 7. <https://doi.org/10.1007/s10584-021-03010-6>
- Railsback, L. B., Liang, F., Brook, G. A., Voarintsoa, N. R. G., Sletten, H. R., Marais, E., et al. (2018). The timing, two-pulsed nature, and variable climatic expression of the 4.2 ka event: A review and new high-resolution stalagmite data from Namibia. *Quaternary Science Reviews*, 186, 78–90. <https://doi.org/10.1016/j.quascirev.2018.02.015>
- Renssen, H. (2022). Climate model experiments on the 4.2 ka event: The impact of tropical sea-surface temperature anomalies and desertification. *The Holocene*, 32(5), 378–389. <https://doi.org/10.1177/09596836221074031>
- Scholz, D., & Hoffmann, D. L. (2011). StalAge – An algorithm designed for construction of speleothem age models. *Quaternary Geochronology*, 6(3–4), 369–382. <https://doi.org/10.1016/j.quageo.2011.02.002>
- Scroton, N., Burns, S. J., McGee, D., Godfrey, L. R., Ranivoharimanana, L., Faina, P., & Tiger, B. H. (2023). Tropical Indian Ocean basin hydroclimate at the Mid-to Late-Holocene transition and the double drying hypothesis. *Quaternary Science Reviews*, 300, 107837. <https://doi.org/10.1016/j.quascirev.2022.107837>
- Sharifi, A., Pourmand, A., Canuel, E. A., Ferer-Tyler, E., Peterson, L. C., Aichner, B., et al. (2015). Abrupt climate variability since the last deglaciation based on a high-resolution, multi-proxy peat record from NW Iran: The hand that rocked the Cradle of Civilization? *Quaternary Science Reviews*, 123, 215–230. <https://doi.org/10.1016/j.quascirev.2015.07.006>
- Takahashi, K., Montecinos, A., Goubanova, K., & Dewitte, B. (2011). ENSO regimes: Reinterpreting the canonical and Modoki El Niño: Reinterpreting ENSO modes. *Geophysical Research Letters*, 38(10). <https://doi.org/10.1029/2011GL047364>
- Theaker, C. M., Carolin, S. A., & Day, C. C. (2024). Borneo stalagmite BA03 high resolution 3.8 kyBP and 4.1 kyBP ENSO proxy windows [Dataset]. *Oxford University Research Archive*. <https://doi.org/10.5287/ora-lrvnxwme0>
- Toth, L. T., & Aronson, R. B. (2019). The 4.2 ka event, ENSO, and coral reef development. *Climate of the Past*, 15(1), 105–119. <https://doi.org/10.5194/cp-15-105-2019>
- Tudhope, A. W., Chilcott, C. P., McCulloch, M. T., Cook, E. R., Chappell, J., Ellam, R. M., et al. (2001). Variability in the El Niño–Southern Oscillation through a glacial-interglacial cycle. *Science*, 291(5508), 1511–1517. <https://doi.org/10.1126/science.1057969>
- Voosen, P. (2018). New geological age comes under fire. *Science*, 361(6402), 537–538. <https://doi.org/10.1126/science.361.6402.537>
- Walker, M., Head, M. J., Berkelhammer, M., Björck, S., Cheng, H., Cwynar, L., et al. (2018). Formal ratification of the subdivision of the Holocene Series/Epoch (Quaternary System/Period): Two new global boundary stratotype sections and Points (GSSPs) and three new stages/subseries. *Episodes*, 41(4), 213–223. <https://doi.org/10.18814/epiugs/2018/018016>
- Wang, D., Li, M., Zhang, S., Xu, Q., & Wu, L. (2022). Spatial and temporal characteristics of the precipitation response to the 4.2 ka event in the Asian summer monsoon region. *Global and Planetary Change*, 214, 103854. <https://doi.org/10.1016/j.gloplacha.2022.103854>

- Watanabe, T. K., Watanabe, T., Yamazaki, A., & Pfeiffer, M. (2019). Oman corals suggest that a stronger winter shamal season caused the Akkadian Empire (Mesopotamia) collapse. *Geology*, 47(12), 1141–1145. <https://doi.org/10.1130/G46604.1>
- Weiss, H., Courty, M.-A., Wetterstrom, W., Guichard, F., Senior, L., Meadow, R., & Curnow, A. (1993). The Genesis and collapse of third millennium north Mesopotamian civilization. *Science*, 261(5124), 995–1004. <https://doi.org/10.1126/science.261.5124.995>
- Woodroffe, C. D., & Gagan, M. K. (2000). Coral microatolls from the central Pacific record late Holocene El Niño. *Geophysical Research Letters*, 27(10), 1511–1514. <https://doi.org/10.1029/2000GL011407>
- Yu, Y., Notaro, M., Liu, Z., Wang, F., Alkolibi, F., Fadda, E., & Bakhrjy, F. (2015). Climatic controls on the interannual to decadal variability in Saudi Arabian dust activity: Toward the development of a seasonal dust prediction model: Saudi Arabian dust prediction. *Journal of Geophysical Research: Atmospheres*, 120(5), 1739–1758. <https://doi.org/10.1002/2014JD022611>